

# **Input Motions for Earthquake Simulator Testing of Electric Substation Equipment (408)**

## **Project Final Report**

**Feng Su, Yuehua Zeng and John G. Anderson**

Seismological Laboratory /174, University of Nevada, Reno, Nevada 89557

## Project Summary

In this project, we have accomplished two major tasks. For the first task, we have developed a method to calculate accelerograms that match a design target spectrum for appropriate earthquake magnitude, distance, and site conditions. Adjustments are made to acceleration-time history records by computing the response spectra and determining the amount of adjustment needed in different period ranges to nearly match the target design spectrum. Fourier spectra are then computed. The Fourier amplitude spectra are adjusted while the Fourier phase spectra are preserved. The inverse Fourier transform is used to re-compute acceleration-time histories. If necessary, the procedure can be iterated to achieve reasonably optimal spectral matching. Velocity- and displacement-time history records and response spectra are computed from the adjusted acceleration-time histories in the usual way. Low-frequency motion introduced by the scaling procedure can be removed by tapering the displacement records to zero at reasonable times based on the shapes of the original acceleration-time histories. Corresponding velocity- and acceleration-time histories are computed by numerical differentiation and final acceleration-response spectra are recomputed.

For the second task, we have examined ground motion response spectra from the recent large earthquakes in California, Japan, Turkey and Taiwan. We have studied the distance, site, and magnitude effect on the shape of the response spectra and compared these response spectra with the standard response spectra specified by the IEEE 693-1997 for high seismic performance level. We found the shape of the response spectra show strong magnitude and site dependency, but weak distance dependency. A larger earthquake generates much more long-period seismic energy than a smaller earthquake. An average soft soil site shows higher amplification of the long-period seismic signal than a rock or stiff soil site. Thus, the normalized spectra from a large earthquake recorded on a soft soil site have the highest likelihood of exceeding IEEE 693-1997 at long periods. By comparing acceleration response spectra with the response spectrum given in IEEE 693-1997 for high seismic performance level, we found the stations that exceed the absolute level of IEEE 693-1997 response spectrum are generally located: 1) very close to the fault rupture trace; 2) near the edge of a fault in a location that experienced a strong directivity effect; 3) on the hanging wall adjacent to the primary fault trace; or 4) at a site that experiences large site amplification. In the low frequency range, the exceedance is usually associated with a larger magnitude earthquake at soft soil sites at near source distance ( $D < 50$  km). For larger earthquakes, exceedance at low frequencies may become more common.

## Introduction

IEEE 693-1997 prescribes standards for the testing of electrical substation equipment. The prescribed spectral shape is shown in Figure 1. The prescribed spectrum is given for two levels, a moderate and high performance level. Those two spectra are normalized to 0.25 g and 0.5 g, respectively. Tests are supposed to assure a factor of safety of 2.0, so for the moderate performance level the test would be performed with a seismogram normalized to the spectrum at 0.5 g, and for the high performance level, the test would ideally be performed to a seismogram matching the spectrum normalized to a peak acceleration of 1.0 g.

## Comparison of IEEE 693-1997 with National Hazard Maps

Figures 2a-l present a comparison of the IEEE 693-1977 spectra with national hazard maps. This is done to evaluate the probabilities that the present standard will be exceeded in various locations within the conterminous United States. Since these maps are available for peak acceleration and for SA with damping of 5% at periods of 0.2s, 0.3s, and 1.0s, Table 1 lists the numerical values of IEEE 693-1977 for those parameters. Map colors of green, yellow, red, and black indicate ground motions below the moderate standard, above the moderate standard but below the high standard, above the high standard but below the high test standard, and above the high test standard, respectively.

**Table 1.**  
**Numerical Values of IEEE 693-1977 Standards for 5% Damping**

Parameter	Moderate Standard	High Standard	High Test
	%g	%g	%g
Peak Acceleration	25	50	100
SA (0.2s)	31.25	62.5	125
SA (0.3s)	31.25	62.5	125
SA (1.0s)	28.6	57.2	114.4

The implications from this part of the study clearly depend on the level of risk that is deemed acceptable to the client. For ordinary structures, the traditional building code has been calibrated to a probability of 10% in 50 years. At this probability, the IEEE moderate standard is adequate for most of the country. However, the high standard is needed in California and western Nevada in all cases, in Seattle for SA(2.0s), and in western Oregon and Washington and in the Yellowstone parabola for SA(0.3 s). For SA(0.2s), in addition to all of these regions it is needed in the New Madrid region and in a small region around Charleston. For SA(0.2s) and SA(0.3s), there are some areas along the San Andreas fault, most notably in San Francisco, where even the high testing standard is exceeded at this probability.

The IBC2000 building code is calibrated from the probabilities of 2% in 50 years rather than 10% in 50 years. At this lower probability of exceedance, according to these maps, there are extensive areas in California, Nevada, coastal Washington and Oregon, and near New Madrid and Charleston, where the high testing standard of the IEEE spectrum is exceeded.

Later this year (2002), the USGS is planning to release a new version of its national hazard maps. It should be expected that the overall pattern of high and low hazard in the US is not changed in the 2002 version. There may be some shift in the level of the hazard, which would modify the maps shown in Figures 2a-1. Although draft versions of the revisions have been circulated, it would be premature to anticipate specific conclusions until the final release has been completed.

### **Project Part I: A Method to Scale Earthquake Records to Match Acceleration Response Spectra for Seismic Testing and Engineering Design**

Earthquake design is often based on recorded earthquake ground motions that have been scaled for the design magnitude and distance and the site geotechnical characteristics. Of course, it is important to select records from the appropriate earthquake mechanism (strike-slip, reverse-slip, or normal-slip earthquakes) for site-specific design. The procedure described in this paper uses Fast Fourier Transforms (FFT) to scale acceleration-time history records in the frequency domain so that they closely match target acceleration response spectra. Subsequent modifications to the scaled acceleration records in the time domain are used to maintain reasonable duration of the ground motion. Acceleration response spectra are recomputed from the scaled and modified records.

Following is a step by step procedure which can be used to scale the earthquake records to match acceleration response spectra for engineering design and analysis. If necessary, iterations are needed for some steps to achieve the best solution. They are noted in the steps summarized below:

Step 1. Using any accepted technique, determine the appropriate design earthquake spectrum for the site.

Step 2. Select from a catalog of recorded earthquakes an acceleration-time history that is appropriate for the source mechanism, site distance, and geotechnical site characteristics.

Step 3. Calculate the velocity- and displacement-time histories, if they are not included in the catalog, and the acceleration response spectrum of the selected earthquake record.

Step 4. Compute the ratios between the target design spectrum (Step 1) and the acceleration response spectrum of the selected earthquake record as a function of frequencies (Step 3).

Step 5. Adjust the selected earthquake acceleration record by (1) applying the spectrum ratios as a function of frequencies determined in Step 4 to the Fourier amplitude spectrum of the record and (2) determining the adjusted acceleration-time history using inverse FFT.

Step 6. Calculate adjusted velocity- and displacement-time histories, and the acceleration response spectrum from the acceleration-time history.

Step 7. Compare the spectrum in Step 6 to the target spectrum in Step 1. Iterate Steps 4 through 6, if necessary.

Step 8. Compare the duration of ground motion calculated in Step 6 to the earthquake recordings in Step 2. In particular, evaluate the displacement-time history calculated in Step 6 to determine if additional tapering is necessary to simulate appropriate duration of the recorded ground motion. In this process, a smooth transition in the taper from 0 to 1 is needed to avoid spurious spikes when differentiating the displacement-time history to obtain velocity and acceleration. For example, a modified cosine taper function, shown below, provides such a smooth transition.

$$f(t) = \begin{cases} [1 - \cos(\pi t / t_b)]/2, & \text{if } t < t_b \\ 1, & \text{if } t_b < t < t_d + t_b \\ [1 + \cos(\pi(t - t_b - t_d)/t_e)]/2, & \text{if } t_b + t_d < t < t_e + t_b + t_d \\ 0, & \text{otherwise} \end{cases} \quad (1)$$

where  $t_b$  is the duration of the taper at the beginning of the record,  $t_d$  is the duration of the ground motion after the beginning taper, and  $t_e$  is the duration of the taper after the end of the ground motion duration.

Step 9. Recompute velocity- and acceleration-time histories, and the response spectrum from the displacement-time history in Step 8.

Step 10. Compare the recomputed response spectrum to the target response spectrum in Step 1. Iterate Steps 4 through 9, if necessary.

### **Example**

The examples shown in Figures 3 and 4 are based on the moderate seismic performance level of IEEE Required Response Spectra 693-1997. The two horizontal components of the target spectra are calculated using the formula given on page 50 of the "IEEE recommended practice for seismic design of substations" (1998). The vertical component of the target spectrum is assumed to be 2/3 of the horizontal level. Thus the designed earthquake ground motions produce 0.5 g and 0.33 g peak accelerations at the horizontal and vertical directions, respectively. We have selected two sets of 3-component strong motion accelerations from the 1978 Tabas, Iran earthquake recorded at the Tabas station

and the 1999 Chi-Chi, Taiwan earthquake recorded at the TCU078 station near the hypocenter, respectively.

The 1978 Tabas earthquake has ruptured the Tabas reverse fault and resulted in a Ms7.4 event. The peak ground acceleration at the Tabas site reached 0.85 g. The record was obtained from the Pacific Earthquake Engineering Research Center web site. It consisted of filtered and corrected acceleration-, velocity-, and displacement-time histories and Fourier amplitude and response spectra. Each record had 1642 points of equally spaced values at a time-step of 0.02 second. Fourier amplitude and response spectra were calculated independently for the procedure described in this report.

The top panel of Figure 3a shows one of the horizontal component acceleration-, velocity-, and displacement-time history records of the Tabas earthquake ground motion observed at station Tabas. The top panel of Figure 3b compared the three component acceleration response spectra with the moderate performance level required response spectra of IEEE Std 693-1997. The lower panel of Figure 3a and 3b shows acceleration-, velocity-, displacement-time histories, and the 3-component response spectra that were scaled using two iterations of Steps 4 through 8 of the procedure described above, respectively. The response spectra closely match the target spectrum and the duration of the ground motion is quite reasonable compared to the original observed seismograms.

The 1999 Chi-Chi earthquake has ruptured the Chelungpu fault and resulted in a Ms7.6 event. The peak ground acceleration at the recording site TCU078 was 0.42 g. The seismograms were recorded and distributed by the Central Weather Bureau of Taiwan. The duration of the records is about 90 second with a sampling time step of 0.005 second. Figure 4a and Figure 4b compare the acceleration-, velocity-, displacement-time histories, and the 3-component response spectra between the original observation and the scaled strong ground motions using two iterations of steps 4 through 8 of the procedure described above. Again the response spectra closely match the target spectrum and the duration of the ground motion is compared to the original seismograms.

For both earthquake ground motions, the scaled displacements through the iteration steps from 4 to 7 have resulted in a significant level of long-period motion lasting beyond the original recording duration. The modification made through step 8 has recovered the duration of the scaled seismograms to a reasonable time length compared to the original ground motion record. Velocity- and acceleration-time histories were calculated by numerical differentiation, and the response spectrum was calculated from the modified acceleration record.

## Discussions and comments

The spectral matching procedure described above provides a useful way to scale historical earthquake records for use in engineering design. Appropriate earthquake source mechanisms, magnitudes, and distances, as well as geotechnical profiles at recording stations, must be considered in the selection of earthquake records. The scaled records must be modified after the target response spectrum has been matched to ensure

that the duration of the scaled records is appropriate when compared to the recorded ground motion. The resulting acceleration-time history records may then be used for engineering analyses and design. The method has been applied successfully to compute scenario ground motion of a  $M_w$  7.5 design earthquake produced by a strike-slip fault at a distance of 18 km from a dam site (Keaton et al., 2000). In that application we have calculated the target response spectrum using the attenuation relation of Abrahamson and Silva (1997).

### **Project Part II: Ground Motion Characteristics from Recent Large Earthquakes**

The importance of response spectra as a means of characterizing the ground motions produced by earthquakes and their effects on structures has long been recognized by engineers and seismologists. Response spectra have played a key role in structural design. Based on representative spectra from recorded motions, standard spectra have been developed over the years. For example, the standard response spectrum specified by the IEEE 693-1997 (Figure 1) is the latest industry standard of seismic design for seismic qualification of electric substations.

### **Data**

We have examined the acceleration response spectra of ground motion data from the recent large destructive earthquakes in California, Japan, Turkey and Taiwan. The earthquakes we analyzed are listed in Table 2. Strong motion data are from Dr. Walter Silva of Pacific Engineering and Analysis, who built the database for Pacific Earthquake Engineering Research Center (PEER) (web site: <http://peer.berkeley.edu/smcat>). We used only a 5% damping, but these results can readily be extended to other values of damping.

**Table 2: Earthquakes used in this study**

Earthquake	Date	M
Cape Mendocino	1992/04/25	7.1
Chi-Chi, Taiwan	1999/09/20	7.6
Duzce, Turkey	1999/11/12	7.1
Kobe, Japan	1995/01/16	6.9
Kocaeli, Turkey	1999/08/17	7.4
Landers, CA	1992/06/28	7.3
Loma Prieta, CA	19989/10/18	6.9
Northridge, CA	1994/01/17	6.7

In order to study the distance, site and magnitude effect on the shape of the response spectra, we divided the data from extensively-recorded earthquakes into several groups with common station site conditions and source-site distances. The source-site distance (D) is defined as the closest distance between the station and rupture surface. The distance is divided into four different ranges,  $D < 20\text{km}$ ,  $20 < D < 50\text{km}$ ,  $50 < D < 100\text{km}$ , and  $D > 100\text{km}$ . The station site classification is defined in Table 3. The number of different groups for Chi-Chi and Northridge earthquakes is listed in Table 4.

**Table 3. Definitions of site classifications**

Site classifications (as used in PEER's database, which is consistent with Geomatrix definition, web site: <http://peer.berkeley.edu/smcat> ):

Site A: Rock site,  $V_s > 600 \text{ mps}$ , or less than 5m of soil over rock.

Site B: Stiff soil site, less than 20m thick of soil over rock,

Site C: Deep narrow soil site, at least more than 20m of soil overlying rock, in a narrow canyon or valley no more than several km wide.

Site D: Deep broad soil site, at least more than 20m of soil overlying rock, in a broad valley,

Site E: Soft deep soil site,  $V_s < 150 \text{ mps}$ .

For Chi-Chi, Taiwan earthquake, the site classification is according to Central Weather Bureau of Taiwan (Lee et al, 2001).

SITE 1: Hard site,

SITE 2: Medium site,

SITE 3: Soft soil site.

**Table 4: Number of data in each group**

<b>Earthquake</b>	D(km) Site	< 20	20~50	50 ~ 100	> 100
Chi-Chi, Taiwan	Site 1	54	52	130	42
	Site 2	42	34	96	38
	Site 3	4	28	28	42
Northridge, California	Site A	4	26	10	
	Site B	8	18	12	
	Site C	10	26	10	
	Site D	24	62	44	

## 1. Distance effect on response spectra

Figure 5 compares average acceleration response spectra at four different distance ranges from the Chi-Chi earthquake. Among different distance groups, the shape of the averaged response spectra are similar, especially for rock sites (Figure 5a). For medium and soft soil sites (Figure 5b and 5c), the average spectra converge at frequencies below 2 Hz. Figure 6 compares average acceleration response spectra for different distance groups from the Norridge earthquake. The general features are similar to those shown in Figure 5, and also consistent among other earthquakes we studied. In general, we think the spectral shape is weakly dependent on distance.

## 2. Site effect on response spectra

Both Chi-Chi and Northridge data have been used again to show the dependence of the average spectral shape on site effect because the abundant data from these two earthquakes. We compared averaged acceleration response spectra for different site categories within the same distance range. We normalized response spectra to a common peak acceleration in order to focus on the comparison of the spectral shape. Figure 7 shows the result for the Chi-Chi earthquake. It is apparent that there is a difference in spectral shapes from different site conditions. In Figure 7a and 7b, which has data with distance less than 50 km, the average spectral amplitudes are much higher at frequencies below 2 Hz for soft soil sites than for stiff soil or rock sites. The difference in spectral shape among different site categories becomes smaller as the distance increases, in Figure 5c and 5d. The difference in spectra at about 1 Hz in Figure 7d, which has data with distance greater than 100km, may be caused by a basin effect from the Taipei basin. That emphasizes that for this and all of the figures in this study, in spite of the abundance of data, there is the potential for systematic bias in the data, and the true uncertainties are much larger than what can be inferred from the statistics of average past observations. Figure 8 shows the comparison of average acceleration spectra of different site categories within the same distance range for Northridge earthquake. The general feature is similar to Figure 7 for the Chi-Chi earthquake, where soft soil sites show higher normalized spectral amplitudes at lower frequency than do stiff or rock sites at near source distance.

Figure 9 plots mean-plus-one standard deviation acceleration spectra shape (84 percentile approximately) of different site categories within the same distance range for Chi-Chi earthquake. As a comparison, the standard response spectrum specified by the IEEE 693-1997 for high seismic performance level was also plotted in the figure. The response spectra from the Chi-Chi earthquake are significantly higher than the IEEE specified response spectra at frequencies between 0.1 and 2 Hz for soft soil sites, for groups with distance less than 50 km. Figure 10 compares 84 percentile acceleration spectra of different site categories within the distance range less than 20 km for Northridge earthquake.

### **3. Earthquake magnitude effect on response spectra**

That different sizes of earthquakes have differently shaped spectra has long been recognized by seismologists. For example, Aki (1967) presented this spectral dependency on earthquake magnitude as a scaling law of the seismic spectrum, and Anderson and Quaas (1988) confirmed it applies to strong motion response spectra. In engineering community, however, design spectra in the past have not generally taken advantage of the magnitude dependency. There is some implicit dependency on the “maximum magnitude” in the IBC 2000 code. Still, there are some instances where knowledge of the “maximum magnitude” threatening the structure may be helpful in that structure’s risk assessment.

A good example to look at magnitude effect on response spectra shape is to compare them among a group of earthquakes with different magnitude recorded at a similar site condition and travel path. Such a plot is shown in Figure 11. It compares response spectra from samples of 6 earthquakes with a range of magnitudes recorded in Guerrero, Mexico (earthquake data are from Anderson and Quaas, 1988). All these earthquakes were recorded on hard rock sites with S-P time of about 3 seconds. The response spectra from all earthquakes were normalized to PGA equals 1 g to enable comparison of the differences in spectra shapes. Consistent with the seismic scaling law, there is a marked increase in spectral amplitudes at lower frequencies as magnitude increases.. At extremely long periods (e.g. T~20 seconds), the amplitude is expected to increase proportional to  $10^M$ . Figure 12 compares response spectra from the Chi-Chi mainshock and an aftershock located right next to the mainshock. Both earthquakes were recorded by a rock site and a soft soil site. The results show the size of the earthquake has a distinct effect on the shape of the response spectra. The largest earthquakes generate more long-period energy.

### **4. Comparisons with IEEE 693-1997**

We have compared the response spectra of the recent strong motion acceleration recordings with the standard response spectra specified by the IEEE 693-1997 for high seismic performance level. These comparisons are shown in Figure 13. Among all the earthquakes we have examined, every event has some cases that the recorded acceleration response spectra have exceeded the IEEE 693-1997 standard for high seismic performance level. That observation, in itself, is not cause for particular alarm, as the exceedances represent the extremes of a phenomenon with a significant stochastic component. We found that those stations that recorded exceedances are generally located at sites that are: 1) very close to the fault rupture trace; 2) near the edge of the fault that suffer strong directivity effect; 3) on the hanging wall adjacent to the primary fault trace; 4) at the site that suffers large site amplification. In the low frequency range, the exceedance is usually associated with a larger magnitude earthquake at soft soil sites at near source distance ( $D < 50$  km). Due to the magnitude effect on response spectra, it is to be expected that for the rare earthquakes with magnitude significantly larger than Chi-Chi (M7.6), exceedances at long periods will be more common.

## **Discussions and Comments**

To summarize the above results, the shape of the seismic response spectra show strong magnitude dependence (Figure 11 and 12). That dependence could be useful for some earthquake resistant design situations. The IEEE spectrum is exceeded by the average spectra at long periods for sites in the softest category (Figure 7 and 9), as a result of soil amplification. However, the magnitude dependence of the spectrum will cause the low frequencies to be amplified relative to the high frequencies for larger earthquakes. The result is that it will be no surprise to see the low frequency part of the spectrum exceeding the IEEE spectrum for all site categories in a significantly larger magnitude earthquake.

## References

- Abrahamson, N.A., and W.J. Silva. "Empirical response spectral attenuation relations for shallow crustal earthquakes". *Seismological Research Letters*. Vol. 68, No. 1 (1997) p. 94-127.
- Aki, K (1967). Scaling law of seismic spectrum. *Journal of Geophy. Res.* Vol. 72, p. 1217-1231.
- Anderson, J. G and R. Quaas (1988). The Mexico earthquake of September 19, 1985 – Effect of magnitude on the character of strong ground motion: An example from the Guerrero, Mexico strong motion network, *Earthquake Spectra*, p. 635-646.
- Keaton J. R., Y. Zeng, and J. G. Anderson (2000). Procedure for scaling earthquake records to match acceleration response spectra for engineering design, submitted to the proceeding papers of the 6th International Conference on Seismic Zonation
- Lee, Chyi-Tyi, Chin-Tung Cheng, Chi-Wen Liao, and Yi-Ben Tsai (2001). Site Classification of Taiwan Free-Field Strong-Motion Stations, BSSA, 91, p 1283-1297.
- Somerville, P.G., N.F. Smith, R.W. Graves, and N.A. Abrahamson. "Modification of empirical strong ground motion attenuation relations to include amplitude and duration effects of rupture directivity". *Seismological Research Letters*. Vol. 68, No. 1 (1997) p. 199-222.

## Figure Captions

Figure 1: The IEEE 693-1997 standard response spectra of high-seismic-performance level. It is the latest industry standard of seismic design for seismic qualification of electric substations. (Slide 1)

Figure 2a. Comparison of the IEEE 693-1997 standards for peak acceleration with the 1997 National Seismic Hazard Maps (Frankel et al, 1997). This map compares the IEEE standard with the national hazard with peak accelerations that have 10% probability of exceedance in 50 years. The map is colored green where the peak acceleration with 10% probability in 50 years is less than the moderate ground motion standard. The map is colored yellow where the peak acceleration with 10% probability in 50 years is more than the moderate standard, but less than the high standard. The map is red where the peak acceleration with 10% probability in 50 years is more than high ground motion standard, but less than the high test standard (i.e. with a factor of safety of 2.0). The map is black where the peak acceleration with 10% probability in 50 years exceeds the high test standard.

Figure 2b. Equivalent of Figure 2a, but compared with peak accelerations with a probability of exceedance of 5% in 50 years.

Figure 2c. Equivalent of Figure 2a, but compared with peak accelerations with a probability of exceedance of 2% in 50 years.

Figure 2d. Equivalent of Figure 2a, but compared with SA(0.2 s) with a probability of exceedance of 10% in 50 years.

Figure 2e. Equivalent of Figure 2a, but compared with SA(0.2 s) with a probability of exceedance of 5% in 50 years.

Figure 2f. Equivalent of Figure 2a, but compared with SA(0.2 s) with a probability of exceedance of 2% in 50 years.

Figure 2g. Equivalent of Figure 2a, but compared with SA(0.3 s) with a probability of exceedance of 10% in 50 years.

Figure 2h. Equivalent of Figure 2a, but compared with SA(0.3 s) with a probability of exceedance of 5% in 50 years.

Figure 2i. Equivalent of Figure 2a, but compared with SA(0.3 s) with a probability of exceedance of 2% in 50 years.

Figure 2j. Equivalent of Figure 2a, but compared with SA(1.0 s) with a probability of exceedance of 10% in 50 years.

Figure 2k. Equivalent of Figure 2a, but compared with SA(1.0 s) with a probability of exceedance of 5% in 50 years.

Figure 2l. Equivalent of Figure 2a, but compared with SA(1.0 s) with a probability of exceedance of 2% in 50 years.

Figure 3a. Top panel shows one of the horizontal component acceleration-, velocity-, and displacement-time history records of the Tabas earthquake ground motion observed at station Tabas. The lower panel shows scaled acceleration-, velocity-, displacement-time histories using two iterations of Steps 4 through 8 of the procedure described in the text.

Figure 3b. Top panel compares the three component acceleration response spectra with the moderate performance level required response spectra of IEEE Std 693-1997. The lower panel compares the scaled 3-component response spectra with the target spectrum of the IEEE recommendation.

Figure 4a. Same as Figure 3a but for the Chi-Chi taiwan earthquake recorded at station TCU078.

Figure 4b. Same as Figure 3b but for the Chi-Chi taiwan earthquake recorded at station TCU078.

Figure 5: Compare average acceleration spectra of the same site category at different distance range for Chi-Chi earthquake. The different distance ranges are D<20km, 20<D<50km; 50<D<100km; D>100km. (a) SITE 1; (b) SITE 2; (c) SITE 3. (Slides 7-9)

Figure 6: Compare average acceleration spectra of the same site category at different distance range for Northridge earthquake. The different distance ranges are D<20km, 20<D<50km, 50<D<100km. (a) site A; (b) site B; (c) site C; (d) site D. (Slides 10-13)

Figure 7: Compare average acceleration spectra of different site categories within the same distance range for Chi-Chi earthquake. The red color for SITE 1, green for SITE 2 and blue for SITE 3. (a) D<20km, (b) 20<D<50km; (c) 50<D<100km; (d) D>100km. (Slides 14-17)

Figure 8: Compare average acceleration spectra of different site categories within the same distance range for Northridge earthquake. The red color for site A, green for site B, blue for site C and light blue for site D. (a) D<20km, (b) 20<D<50km; (c) 50<D<100km. (Slides 22-24)

Figure 9: Compare 84 percentile acceleration spectra of different site categories within the same distance range for Chi-Chi earthquake. The red color for SITE 1, green for SITE 2 and blue for SITE 3. (a) D<20km, (b) 20<D<50km; (c) 50<D<100km; (d) D>100km. (Slides 18-21)

Figure 10: Compare 84 percentile acceleration spectra of different site categories within the same distance range ( $D < 20\text{km}$ ) for Northridge earthquake. The red color for site A, green for site B, blue for site C and light blue for site D. (Slide 25)

Figure 11: Compare response spectra from samples of earthquakes with a range of magnitudes recorded on rock sites in Guerrero, Mexico. (Slide 26)

Figure 12: Compare response spectra from the Chi-Chi mainshock and a aftershock located right next to the mainshock recorded at a rock site (blue line) and a soft soil site (red line). (Slide 27)

Figure 13: The acceleration response spectra from recent large earthquakes in Taiwan, Turkey, Japan, and California (see Table 2 for the list of the earthquakes). The figures show only those acceleration response spectra, which have  $\text{Sa}$  values exceeded the IEEE-693-1997 standard for high seismic performance level.

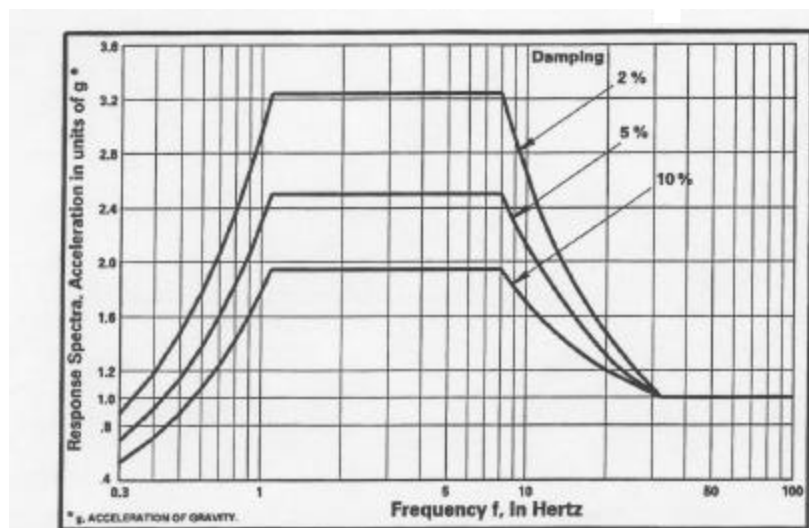


Figure 4—High seismic performance level

Figure 1: The IEEE 693-1997 standard response spectra of high-seismic -performance level. It is the latest industry standard of seismic design for seismic qualification of electric substations.

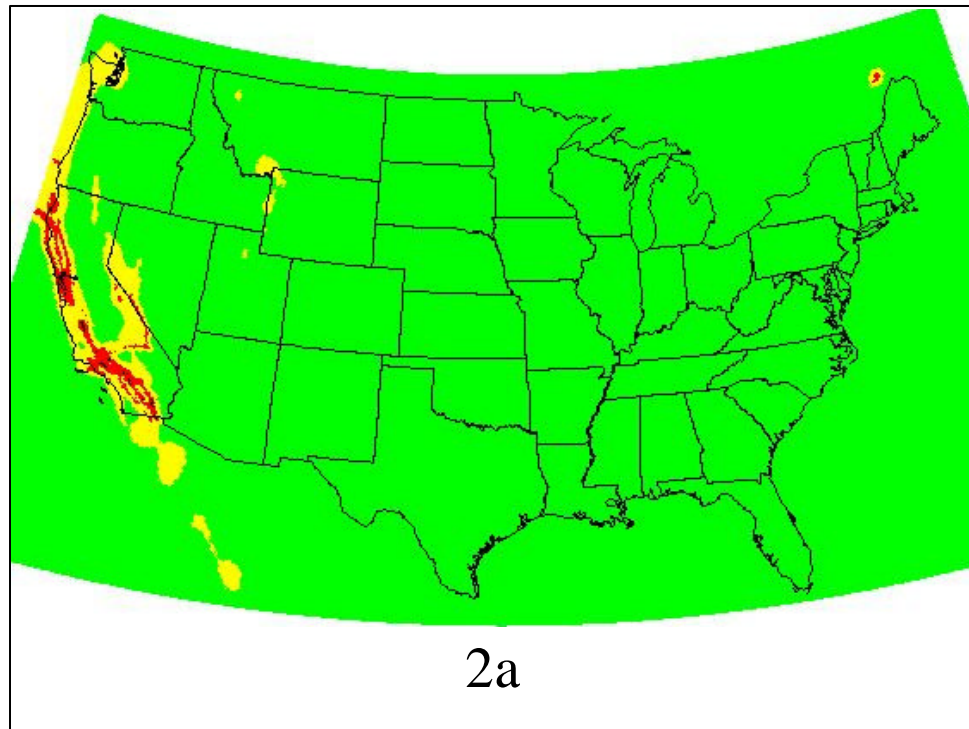


Figure 2a. Comparison of the IEEE 693-1997 standards for peak acceleration with the 1997 National Seismic Hazard Maps (Frankel et al, 1997). This map compares the IEEE standard with the national hazard with peak accelerations that have 10% probability of exceedance in 50 years. The map is colored green where the peak acceleration with 10% probability in 50 years is less than the moderate ground motion standard. The map is colored yellow where the peak acceleration with 10% probability in 50 years is more than the moderate standard, but less than the high standard. The map is red where the peak acceleration with 10% probability in 50 years is more than high ground motion standard, but less than the high test standard (i.e. with a factor of safety of 2.0). The map is black where the peak acceleration with 10% probability in 50 years exceeds the high test standard.

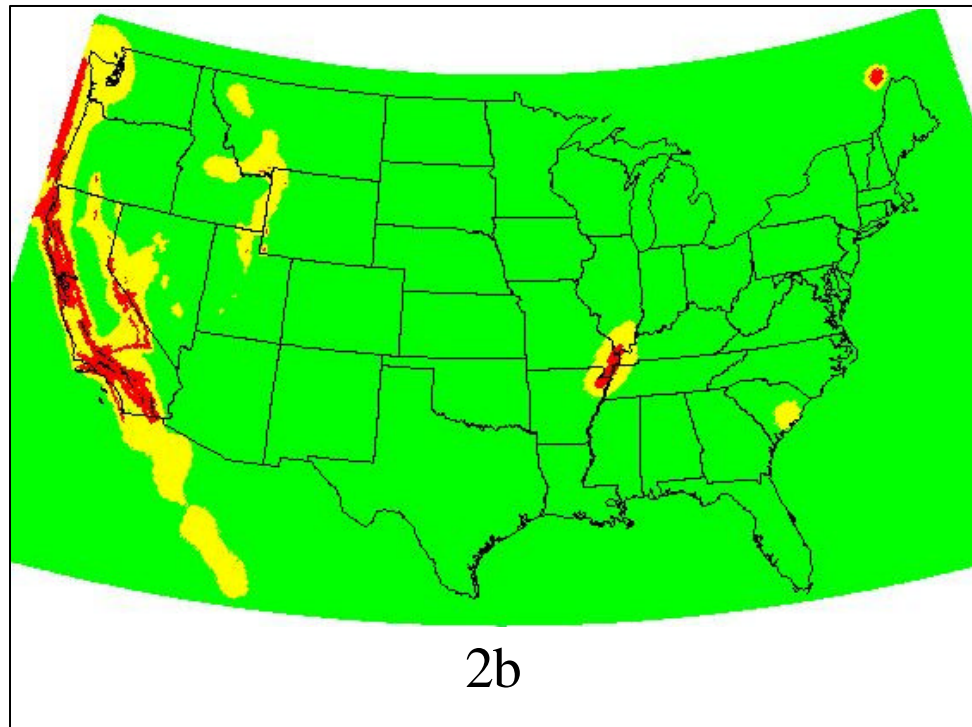


Figure 2b. Equivalent of Figure 2a, but compared with peak accelerations with a probability of exceedance of 5% in 50 years.

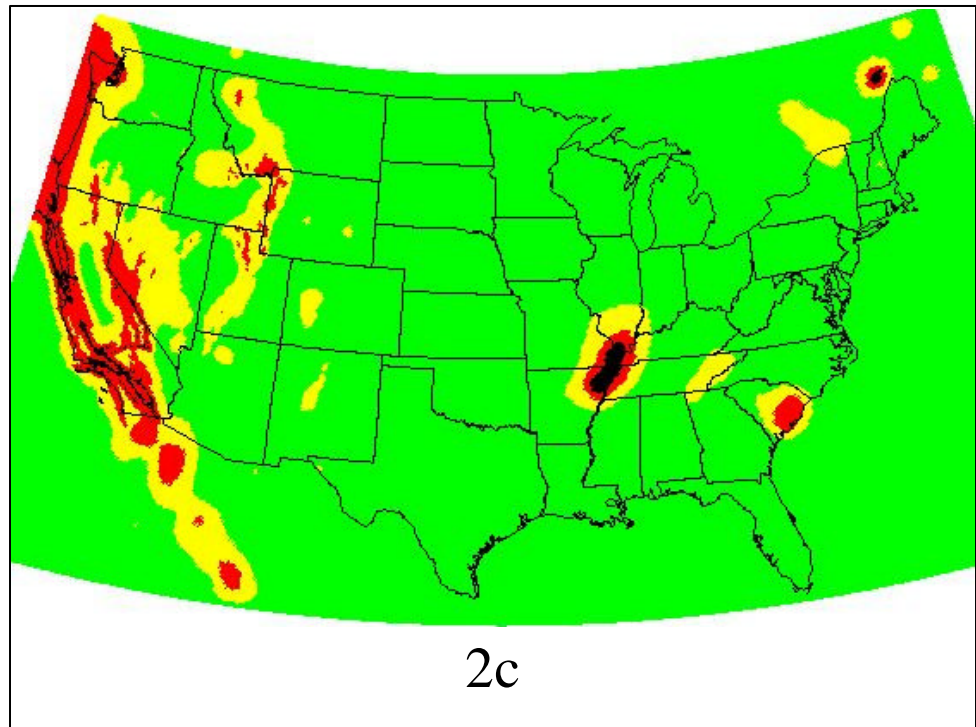
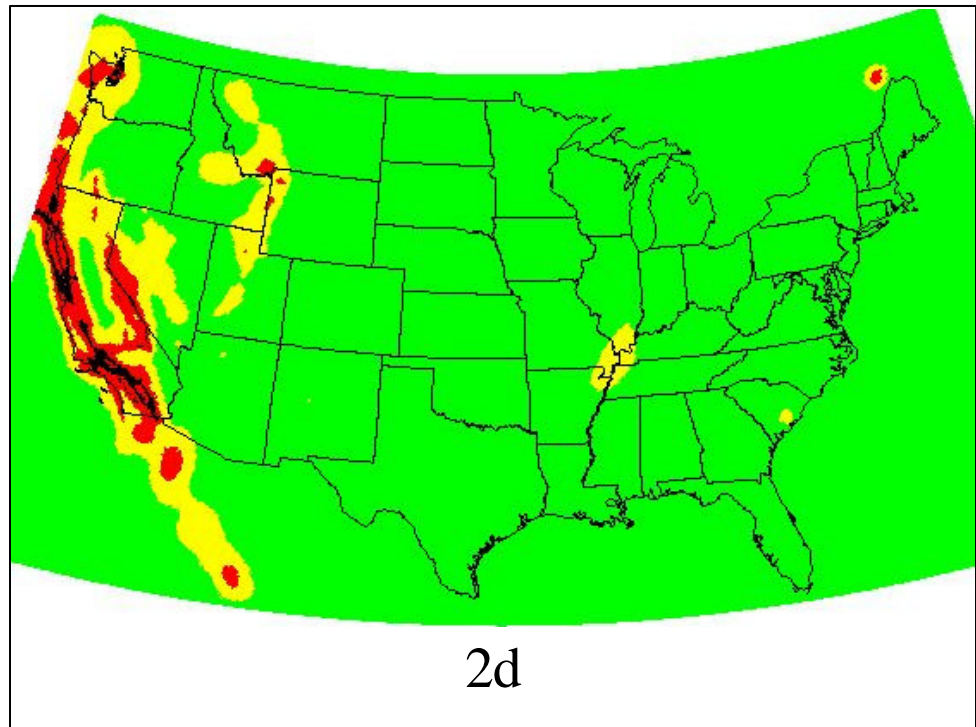
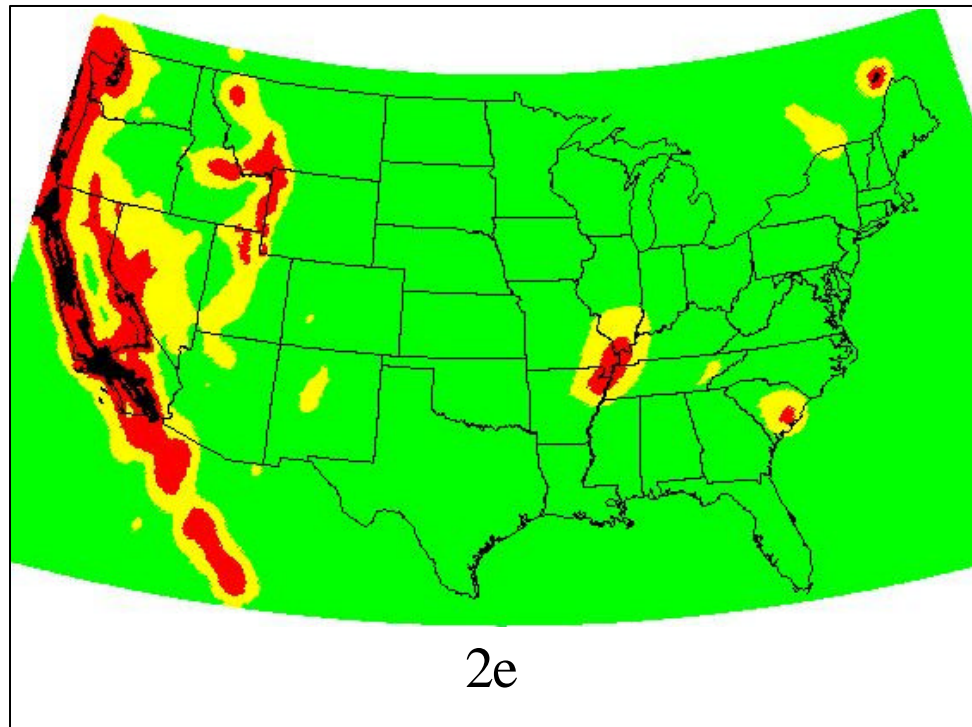


Figure 2c. Equivalent of Figure 2a, but compared with peak accelerations with a probability of exceedance of 2% in 50 years.



**Figure 2d.** Equivalent of Figure 2a, but compared with SA(0.2 s) with a probability of exceedance of 10% in 50 years.



**Figure 2e.** Equivalent of Figure 2a, but compared with SA(0.2 s) with a probability of exceedance of 5% in 50 years.

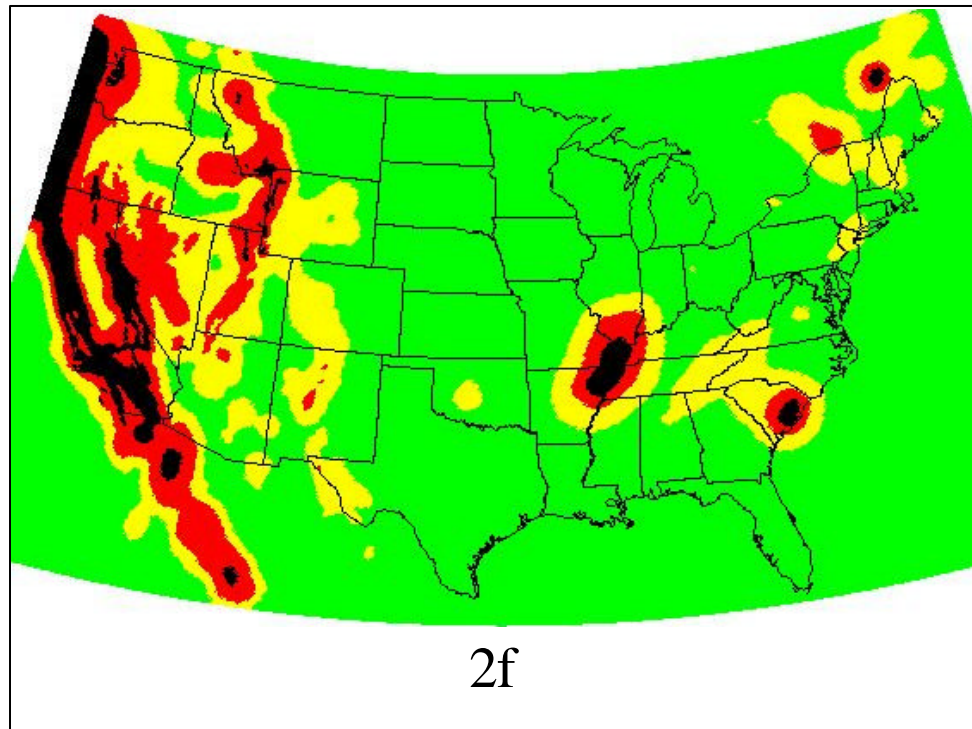


**Figure 2f.** Equivalent of Figure 2a, but compared with SA(0.2 s) with a probability of exceedance of 2% in 50 years.

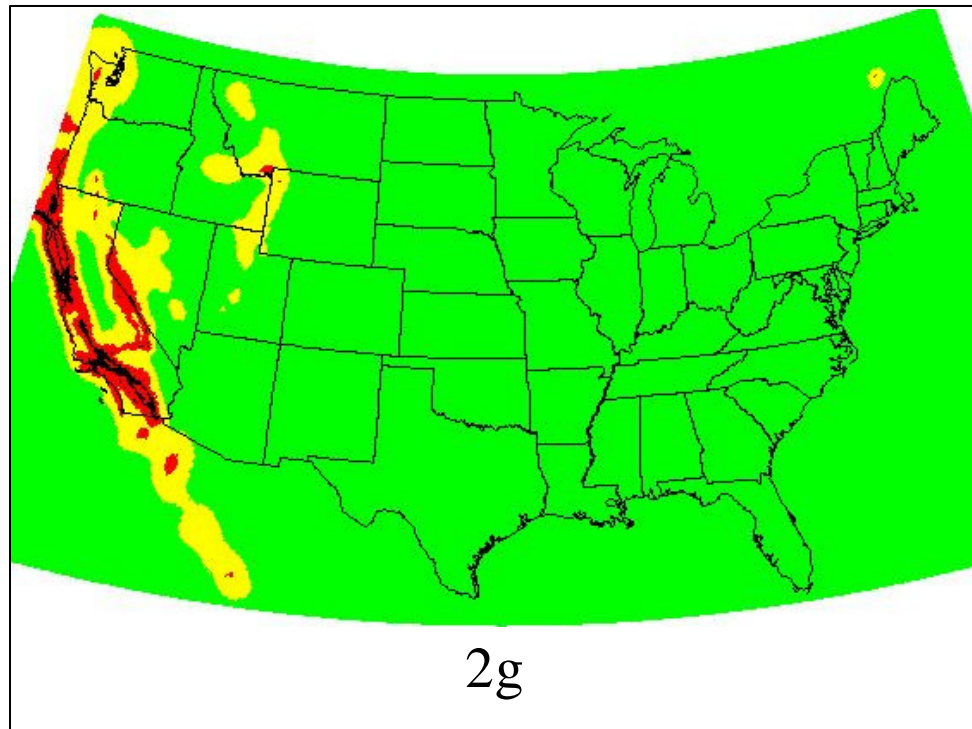


**Figure 2g.** Equivalent of Figure 2a, but compared with SA(0.3 s) with a probability of exceedance of 10% in 50 years.

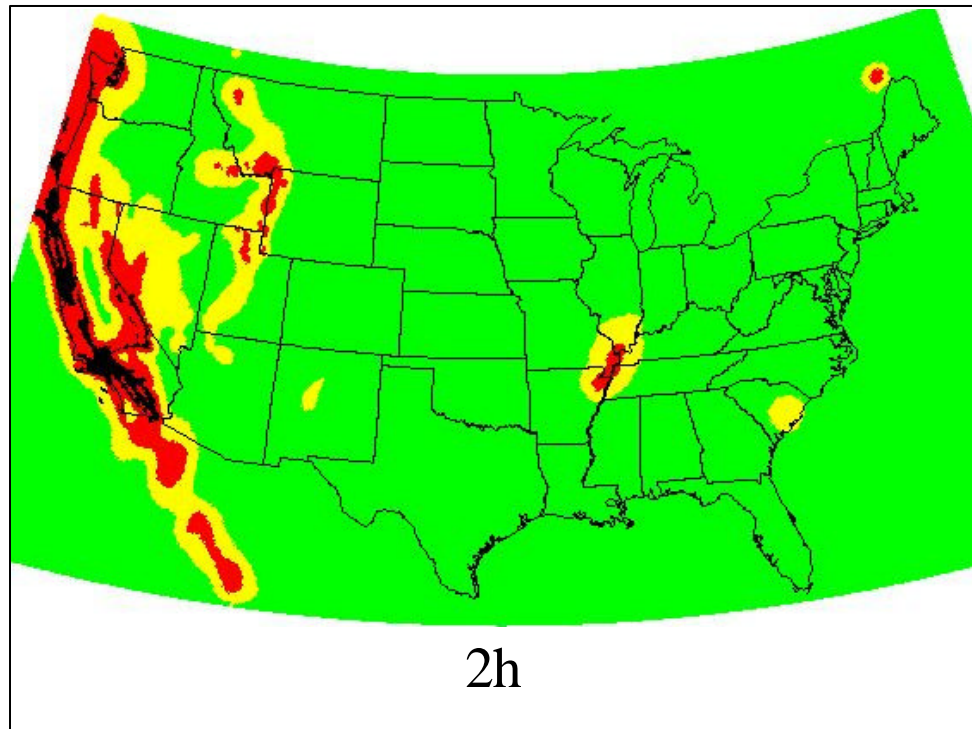


**Figure 2h.** Equivalent of Figure 2a, but compared with SA(0.3 s) with a probability of exceedance of 5% in 50 years.

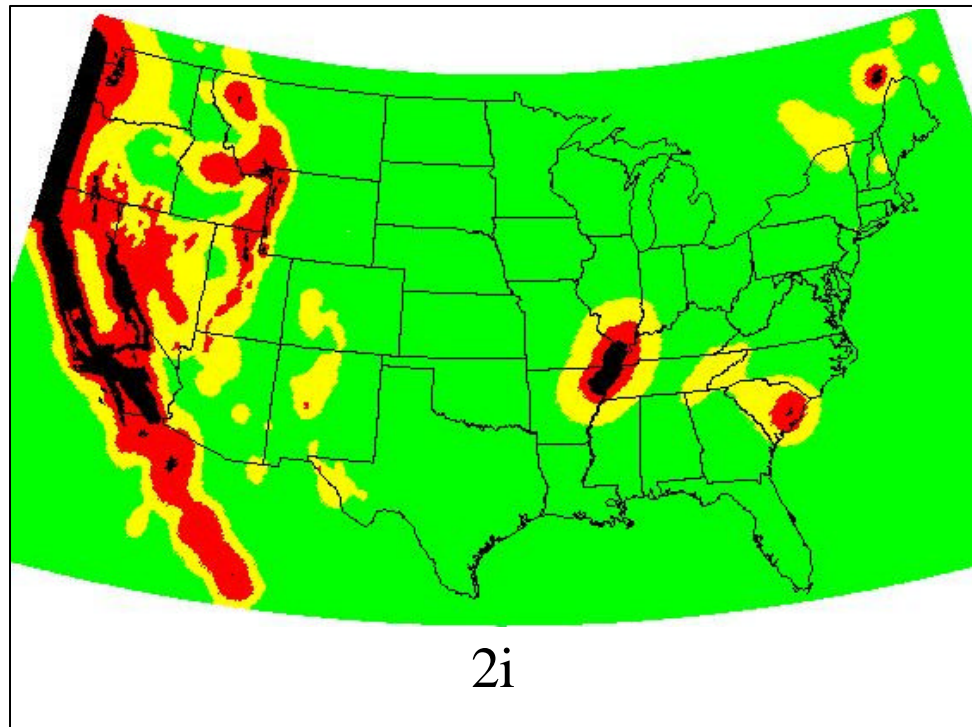
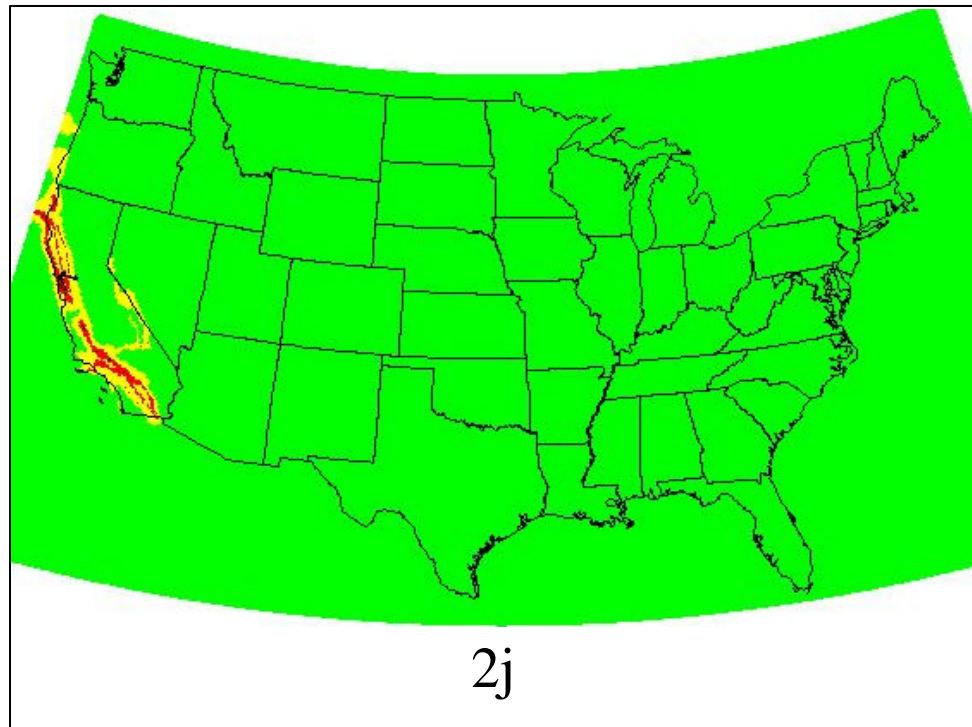


**Figure 2i.** Equivalent of Figure 2a, but compared with SA(0.3 s) with a probability of exceedance of 2% in 50 years.



2j

**Figure 2j.** Equivalent of Figure 2a, but compared with SA(1.0 s) with a probability of exceedance of 10% in 50 years.

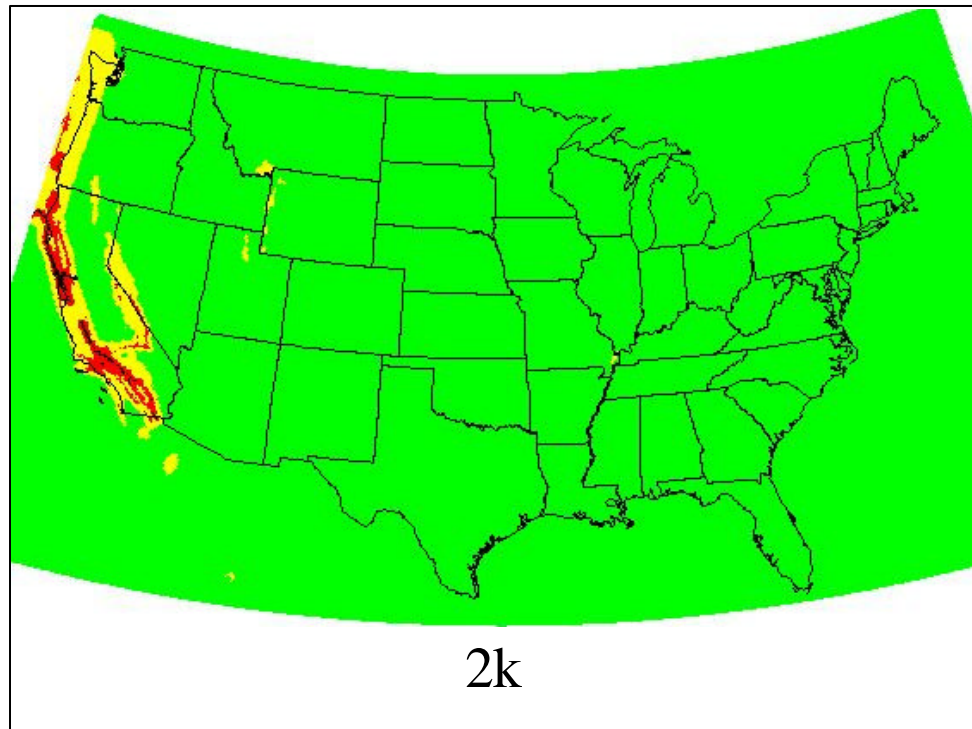


**Figure 2k.** Equivalent of Figure 2a, but compared with SA(1.0 s) with a probability of exceedance of 5% in 50 years.

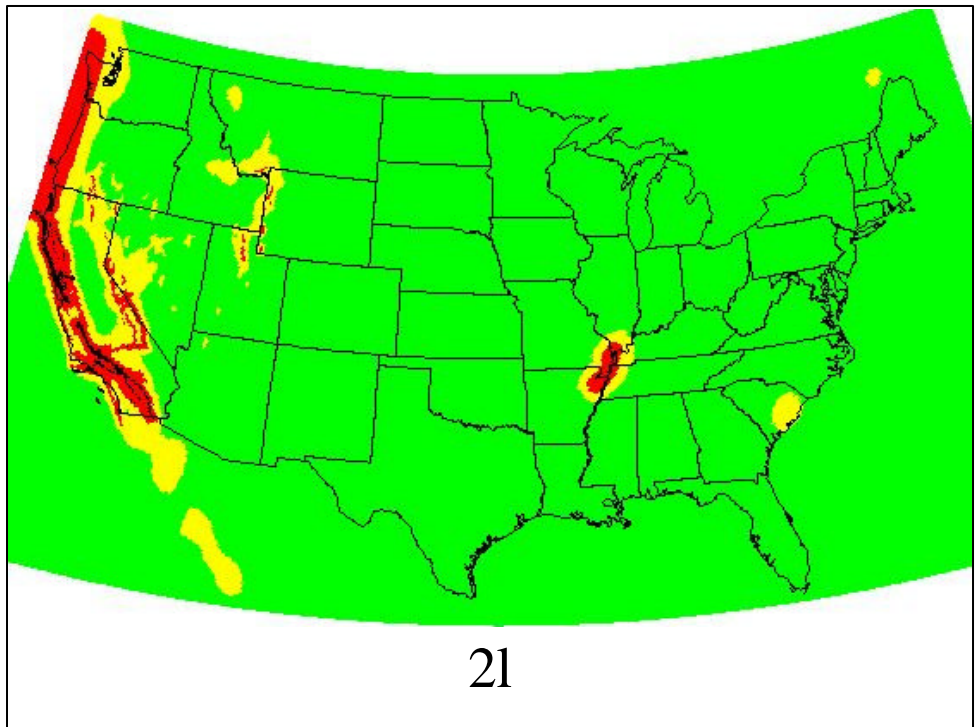


**Figure 2l. Equivalent of Figure 2a, but compared with SA(1.0 s) with a probability of exceedance of 2% in 50 years.**

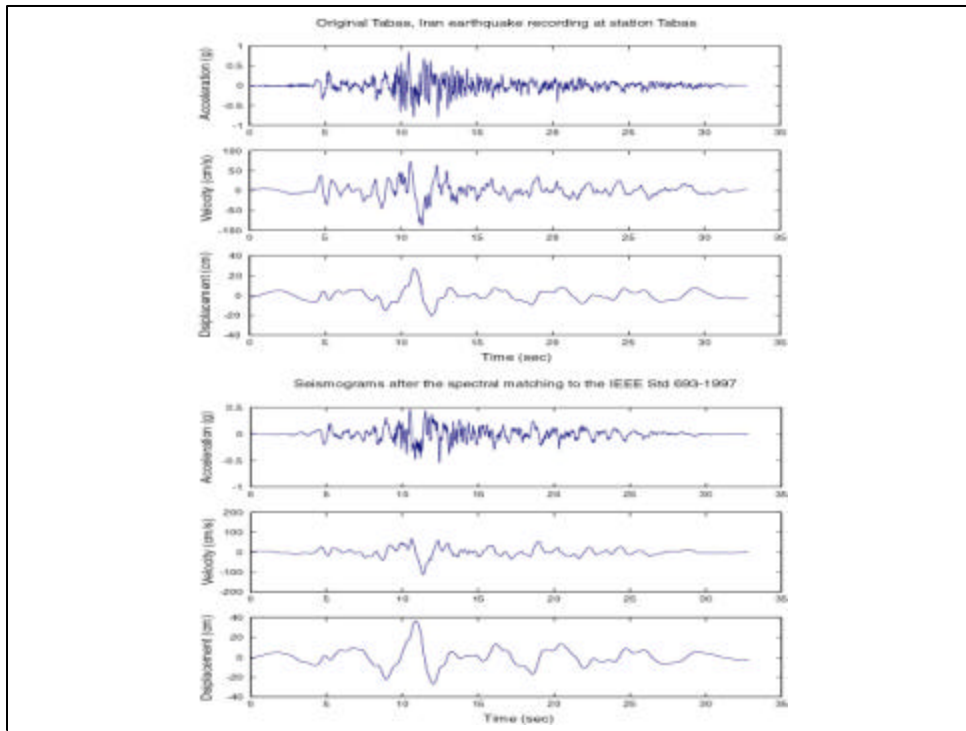


**Figure 3a.** Top panel shows one of the horizontal component acceleration-, velocity-, and displacement-time history records of the Tabas earthquake ground motion observed at station Tabas. The lower panel shows scaled acceleration -, velocity-, displacement-time histories using two iterations of Steps 4 through 8 of the procedure described in the text.

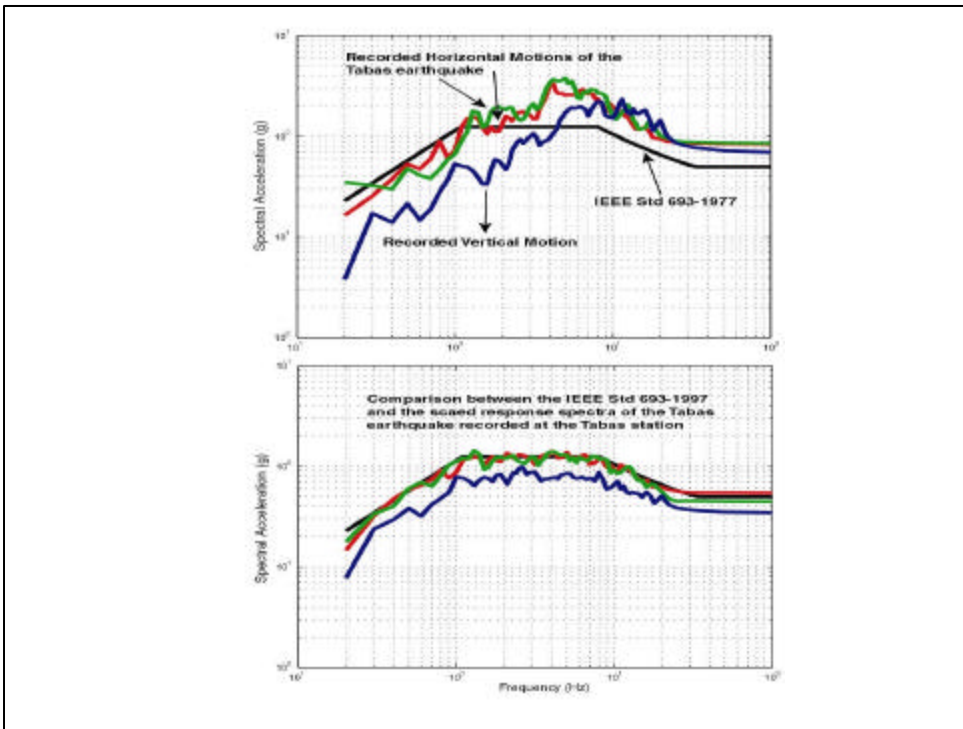


**Figure 3b.** Top panel compares the three component acceleration response spectra with the moderate performance level required response spectra of IEEE Std 693-1997. The lower panel compares the scaled 3-component response spectra with the target spectrum of the IEEE recommendation.

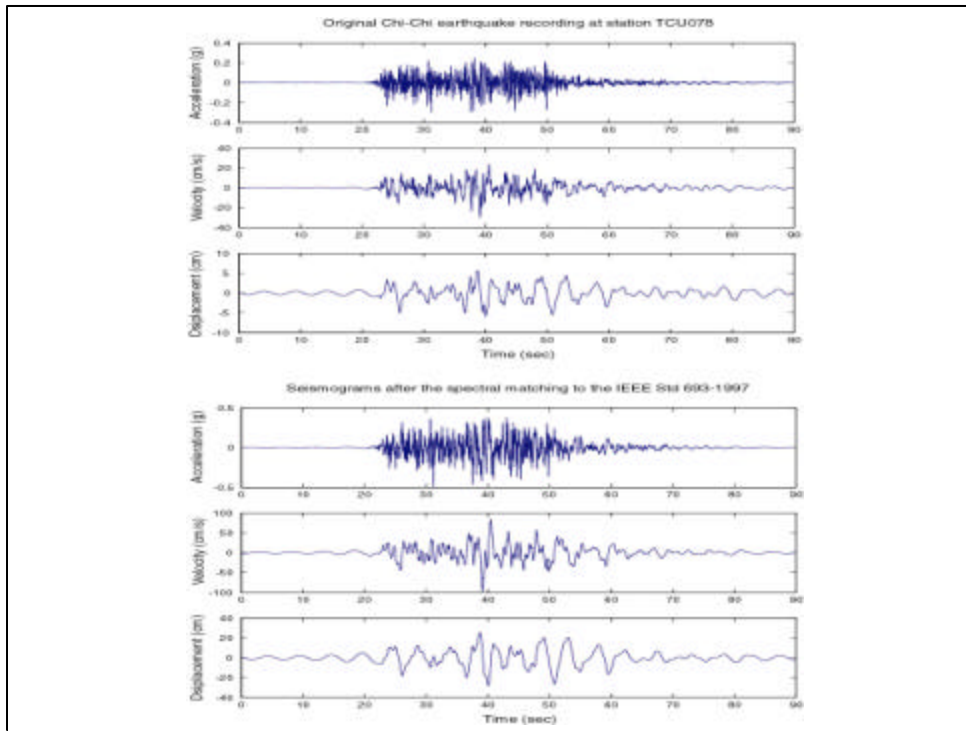


**Figure 4a.** Same as Figure 3a but for the Chi-Chi taiwan earthquake recorded at station TCU078.

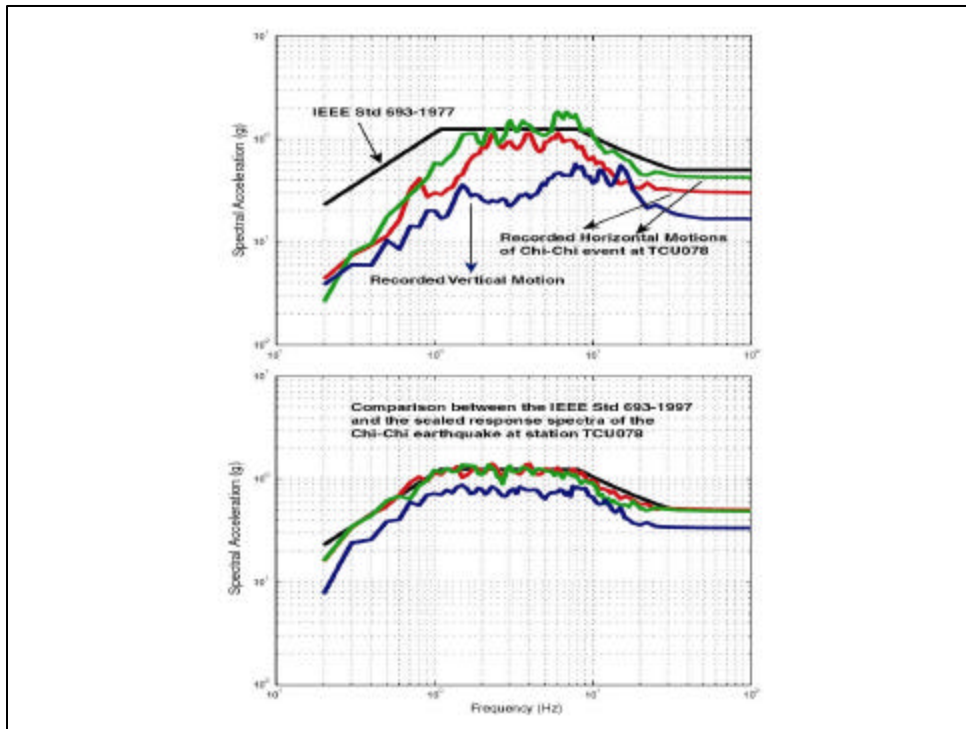


**Figure 4b.** Same as Figure 3b but for the Chi-Chi taiwan earthquake recorded at station TCU078.

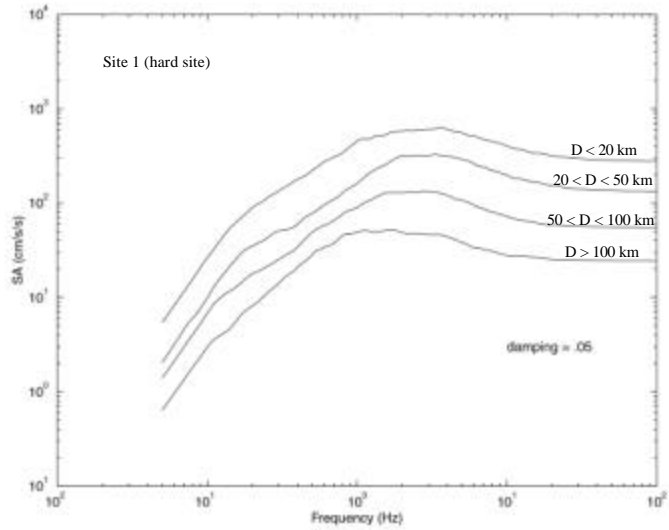


Figure 5a: Compare average acceleration spectra of the same site category at different distance range for Chi-Chi earthquake. The different distance ranges are  $D < 20\text{km}$ ,  $20 < D < 50\text{km}$ ;  $50 < D < 100\text{km}$ ;  $D > 100\text{km}$ . (a) SITE 1; (b) SITE 2; (c) SIT E 3.

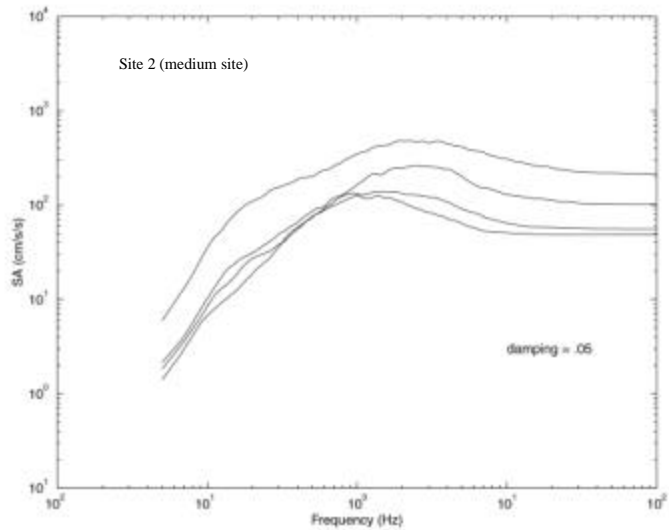


Figure 5b: Compare average acceleration spectra of the same site category at different distance range for Chi-Chi earthquake. The different distance ranges are  $D < 20\text{km}$ ,  $20 < D < 50\text{km}$ ;  $50 < D < 100\text{km}$ ;  $D > 100\text{km}$ . (a) SITE 1; (b) SITE 2; (c) SIT E 3.

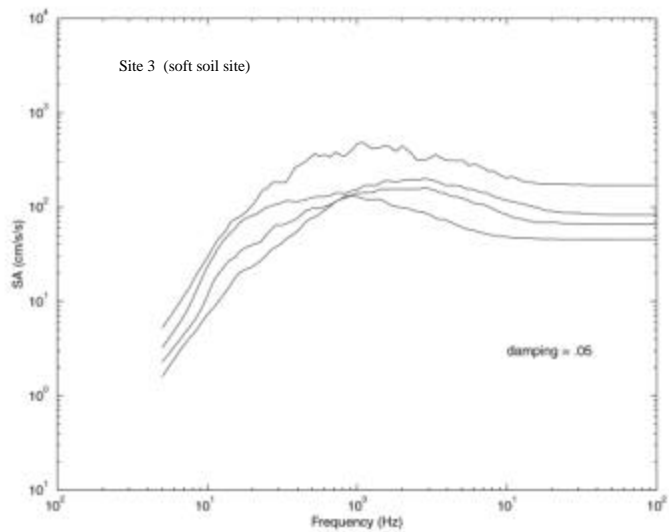


Figure 5c: Compare average acceleration spectra of the same site category at different distance range for Chi-Chi earthquake. The different distance ranges are  $D < 20\text{km}$ ,  $20 < D < 50\text{km}$ ;  $50 < D < 100\text{km}$ ;  $D > 100\text{km}$ . (a) SITE 1; (b) SITE 2; (c) SITE 3.

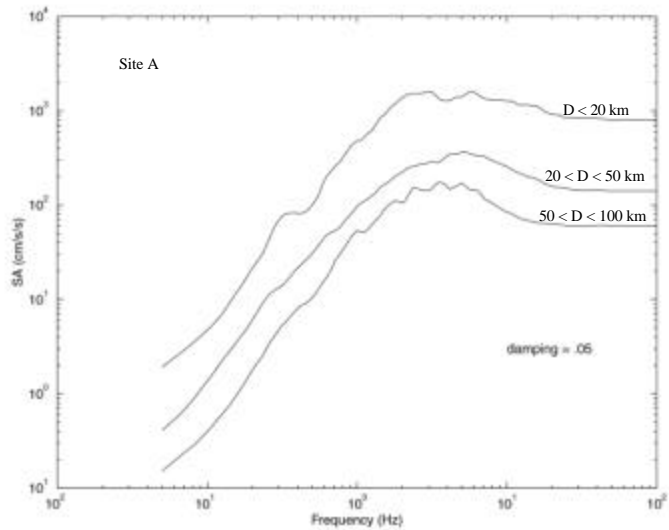


Figure 6a: Compare average acceleration spectra of the same site category at different distance range for Northridge earthquake. The different distance ranges are  $D < 20\text{km}$ ,  $20 < D < 50\text{km}$ ,  $50 < D < 100\text{km}$ . (a) site A; (b) site B; (c) site C; (d) site D.

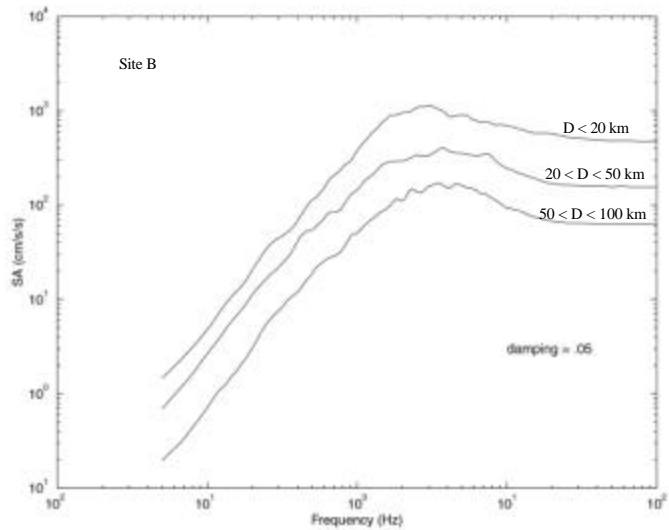


Figure 6b: Compare average acceleration spectra of the same site category at different distance range for Northridge earthquake. The different distance ranges are  $D < 20\text{km}$ ,  $20 < D < 50\text{km}$ ,  $50 < D < 100\text{km}$ . (a) site A; (b) site B; (c) site C; (d) site D.

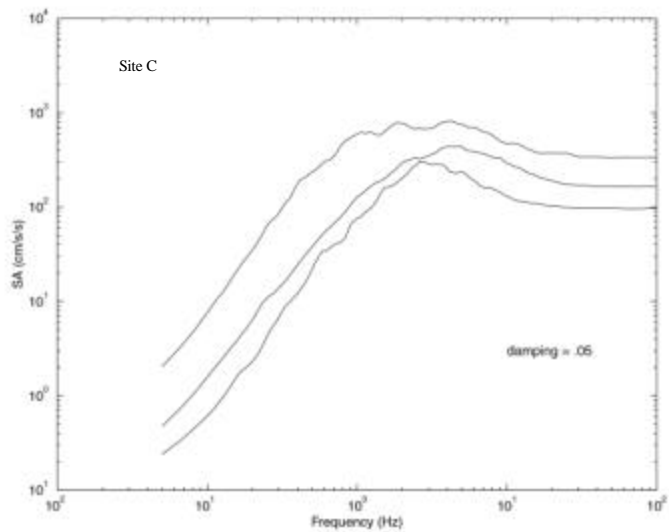


Figure 6c: Compare average acceleration spectra of the same site category at different distance range for Northridge earthquake. The different distance ranges are  $D < 20\text{km}$ ,  $20 < D < 50\text{km}$ ,  $50 < D < 100\text{km}$ . (a) site A; (b) site B; (c) site C; (d) site D.

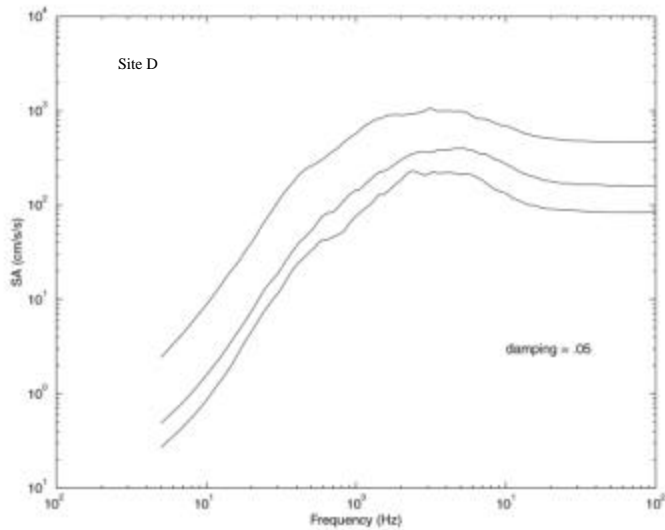


Figure 6d: Compare average acceleration spectra of the same site category at different distance range for Northridge earthquake. The different distance ranges are  $D < 20\text{km}$ ,  $20 < D < 50\text{km}$ ,  $50 < D < 100\text{km}$ . (a) site A; (b) site B; (c) site C; (d) site D.

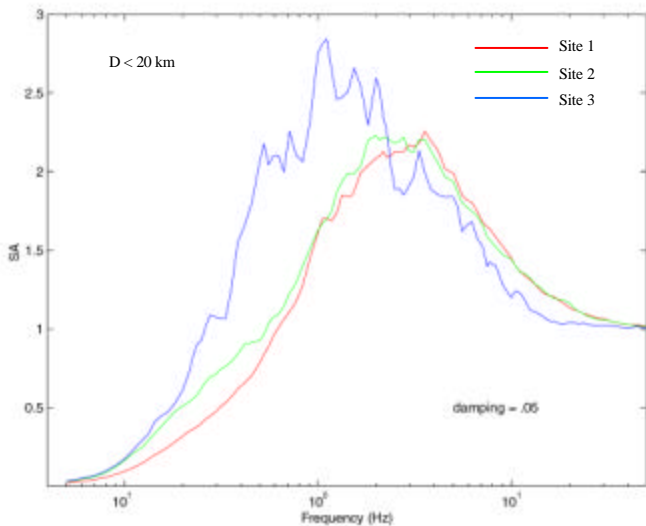


Figure 7a: Compare average acceleration spectra of different site categories within the same distance range for Chi-Chi earthquake. The red color for SITE 1, green for SITE 2 and blue for SITE 3. (a)  $D < 20\text{ km}$ , (b)  $20 < D < 50\text{ km}$ ; (c)  $50 < D < 100\text{ km}$ ; (d)  $D > 100\text{ km}$ .

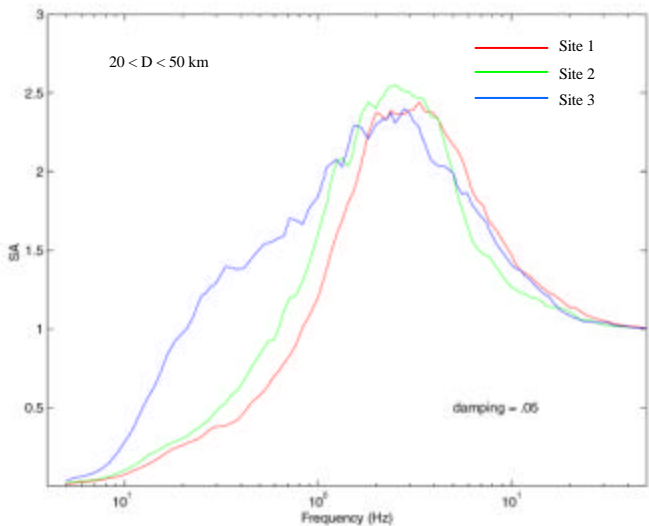


Figure 7b: Compare average acceleration spectra of different site categories within the same distance range for Chi-Chi earthquake. The red color for SITE 1, green for SITE 2 and blue for SITE 3. (a)  $D < 20\text{km}$ , (b)  $20 < D < 50\text{km}$ ; (c)  $50 < D < 100\text{km}$ ; (d)  $D > 100\text{km}$ .

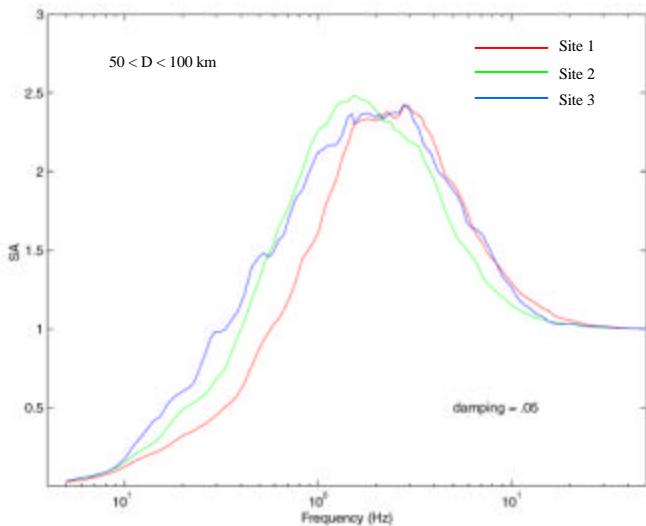


Figure 7c: Compare average acceleration spectra of different site categories within the same distance range for Chi-Chi earthquake. The red color for SITE 1, green for SITE 2 and blue for SITE 3. (a)  $D < 20\text{km}$ , (b)  $20 < D < 50\text{km}$ ; (c)  $50 < D < 100\text{km}$ ; (d)  $D > 100\text{km}$ .

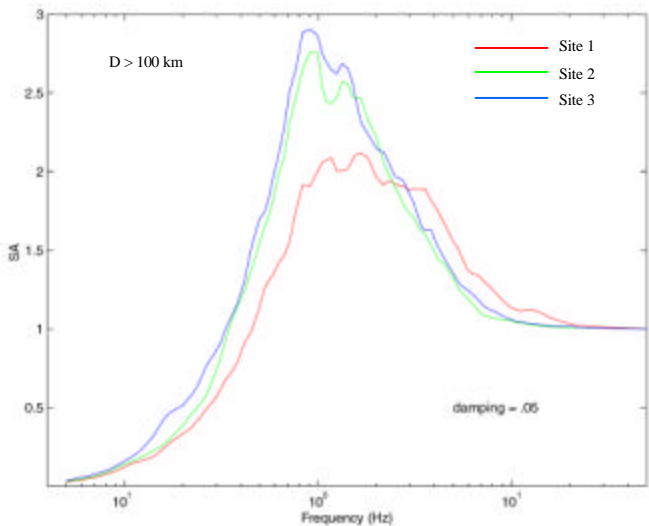


Figure 7d: Compare average acceleration spectra of different site categories within the same distance range for Chi-Chi earthquake. The red color for SITE 1, green for SITE 2 and blue for SITE 3. (a)  $D < 20\text{km}$ , (b)  $20 < D < 50\text{km}$ ; (c)  $50 < D < 100\text{km}$ ; (d)  $D > 100\text{km}$ .

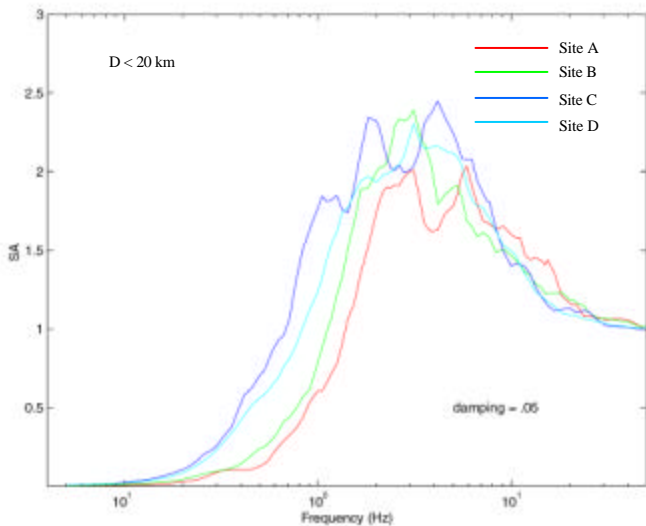


Figure 8a: Compare average acceleration spectra of different site categories within the same distance range for Northridge earthquake. The red color for site A, green for site B, blue for site C and light blue for site D. (a)  $D < 20\text{km}$ , (b)  $20 < D < 50\text{km}$ ; (c)  $50 < D < 100\text{km}$ .

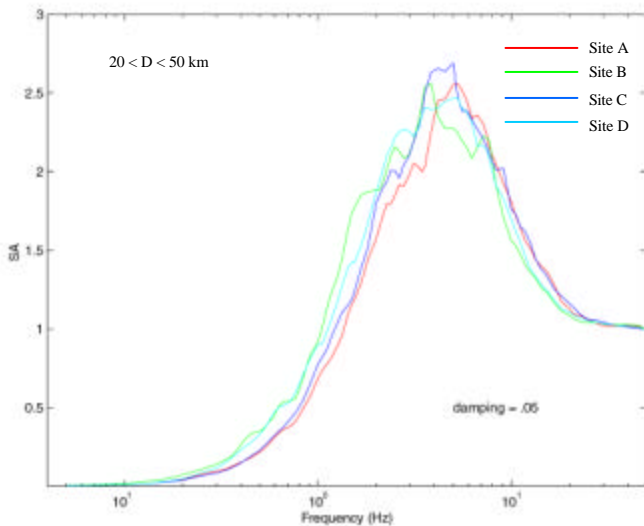


Figure 8b: Compare average acceleration spectra of different site categories within the same distance range for Northridge earthquake. The red color for site A, green for site B, blue for site C and light blue for site D. (a)  $D < 20$ km, (b)  $20 < D < 50$ km; (c)  $50 < D < 100$ km.

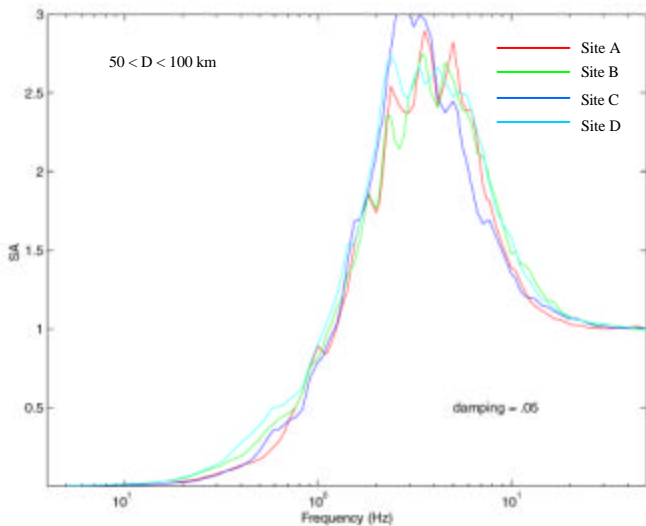


Figure 8c: Compare average acceleration spectra of different site categories within the same distance range for Northridge earthquake. The red color for site A, green for site B, blue for site C and light blue for site D. (a)  $D < 20\text{km}$ , (b)  $20 < D < 50\text{km}$ ; (c)  $50 < D < 100\text{km}$ .

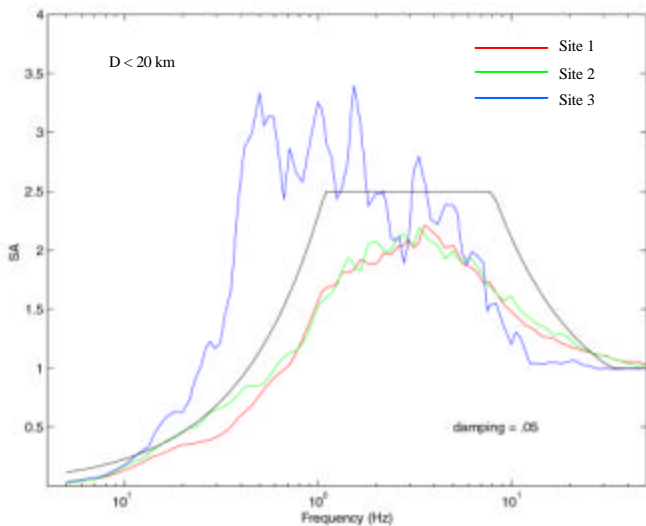


Figure 9a: Compare 84 percentile acceleration spectra of different site categories within the same distance range for Chi-Chi earthquake. The red color for SITE 1, green for SITE 2 and blue for SITE 3. (a)  $D < 20\text{ km}$ , (b)  $20 < D < 50\text{ km}$ ; (c)  $50 < D < 100\text{ km}$ ; (d)  $D > 100\text{ km}$ .

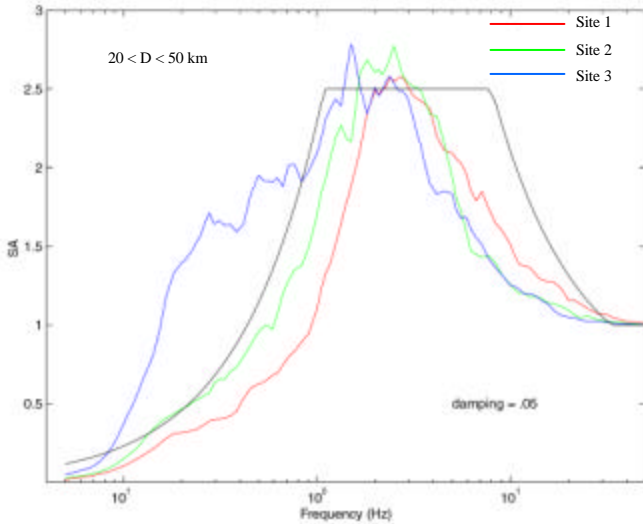


Figure 9b: Compare 84 percentile acceleration spectra of different site categories within the same distance range for Chi-Chi earthquake. The red color for SITE 1, green for SITE 2 and blue for SITE 3. (a)  $D < 20\text{km}$ , (b)  $20 < D < 50\text{km}$ ; (c)  $50 < D < 100\text{km}$ ; (d)  $D > 100\text{km}$ .

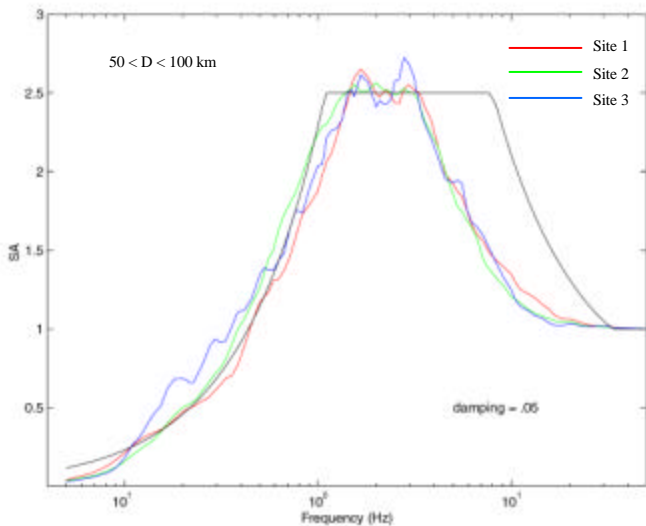


Figure 9c: Compare 84 percentile acceleration spectra of different site categories within the same distance range for Chi-Chi earthquake. The red color for SITE 1, green for SITE 2 and blue for SITE 3. (a)  $D < 20\text{km}$ , (b)  $20 < D < 50\text{km}$ ; (c)  $50 < D < 100\text{km}$ ; (d)  $D > 100\text{km}$ .

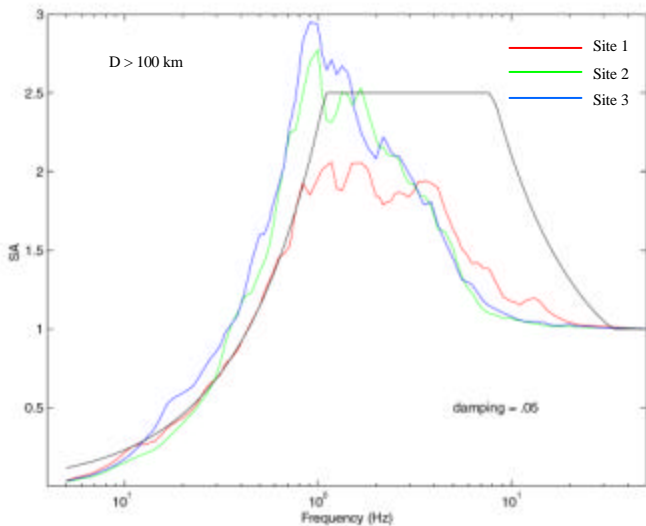


Figure 9d: Compare 84 percentile acceleration spectra of different site categories within the same distance range for Chi-Chi earthquake. The red color for SITE 1, green for SITE 2 and blue for SITE 3. (a)  $D < 20\text{km}$ , (b)  $20 < D < 50\text{km}$ ; (c)  $50 < D < 100\text{km}$ ; (d)  $D > 100\text{km}$ .

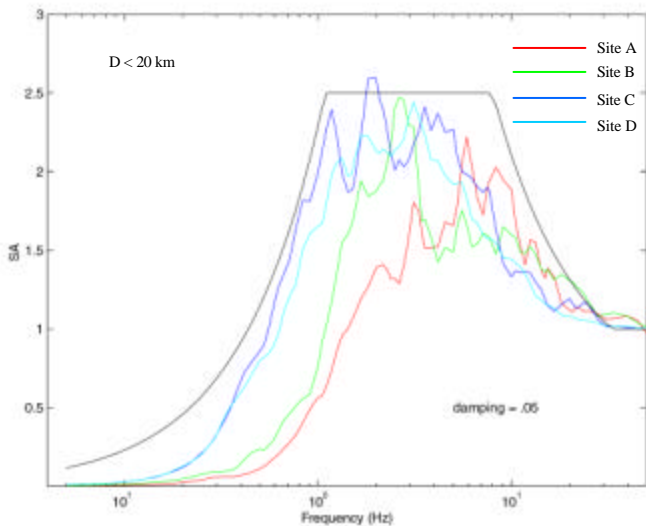


Figure 10: Compare 84 percentile acceleration spectra of different site categories within the same distance range ( $D < 20\text{ km}$ ) for Northridge earthquake. The red color for site A, green for site B, blue for site C and light blue for site D.

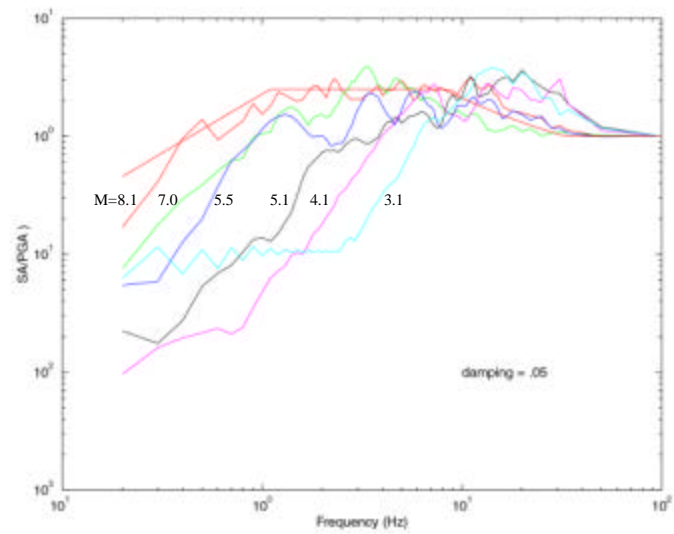


Figure 11: Response spectra from samples of earthquakes with a range of magnitudes recorded on rock sites in Guerrero, Mexico.

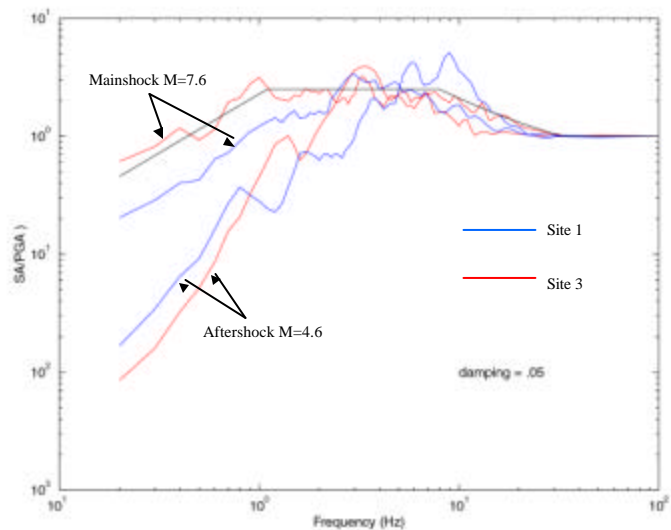


Figure 12: Compare response spectra from the Chi-Chi mainshock and a aftershock located right next to the mainshock recorded at a rock site (blue line) and a soft soil site (red line).

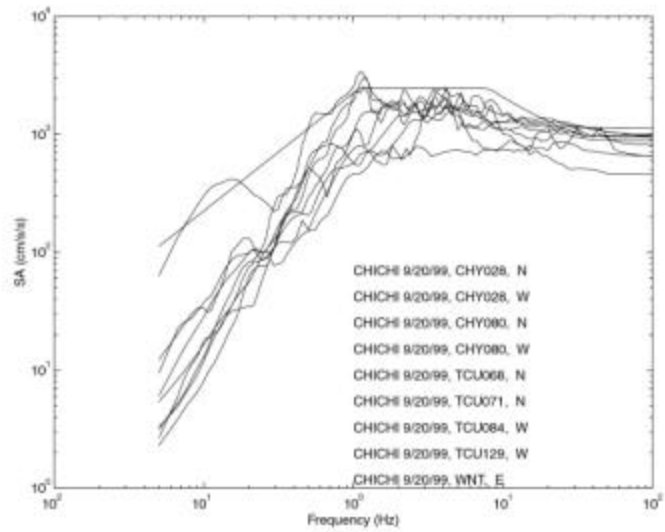


Figure 13a: The acceleration response spectra from recent large earthquakes in Taiwan, Turkey, Japan, and California (see Table 2 for the list of the earthquakes). The figures show only those acceleration response spectra, which have Sa values exceeded the IEEE-693-1997 standard for high seismic performance level.

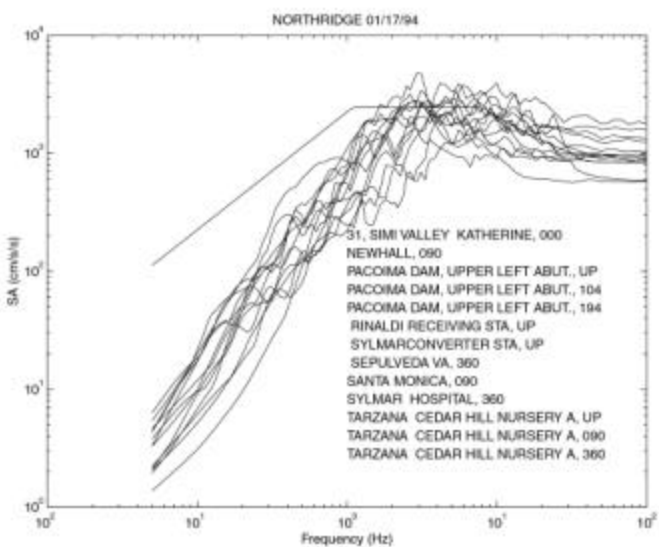


Figure 13b: The acceleration response spectra from recent large earthquakes in Taiwan, Turkey, Japan, and California (see Table 2 for the list of the earthquakes). The figures show only those acceleration response spectra, which have Sa values exceeded the IEEE-693-1997 standard for high seismic performance level.

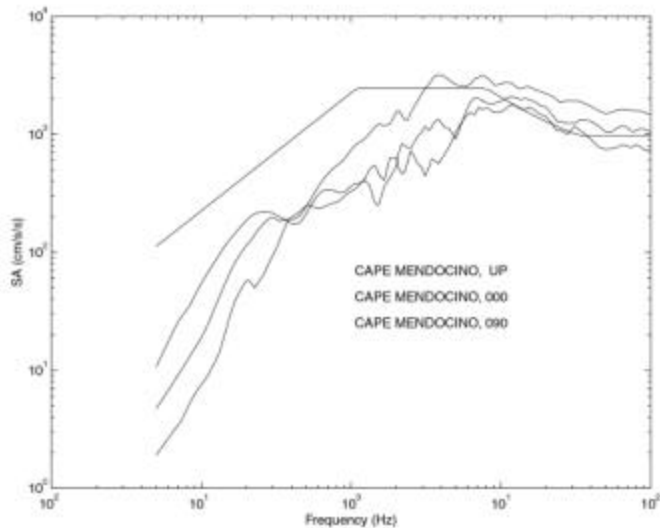


Figure 13c: The acceleration response spectra from recent large earthquakes in Taiwan, Turkey, Japan, and California (see Table 2 for the list of the earthquakes). The figures show only those acceleration response spectra, which have Sa values exceeded the IEEE-693-1997 standard for high seismic performance level.

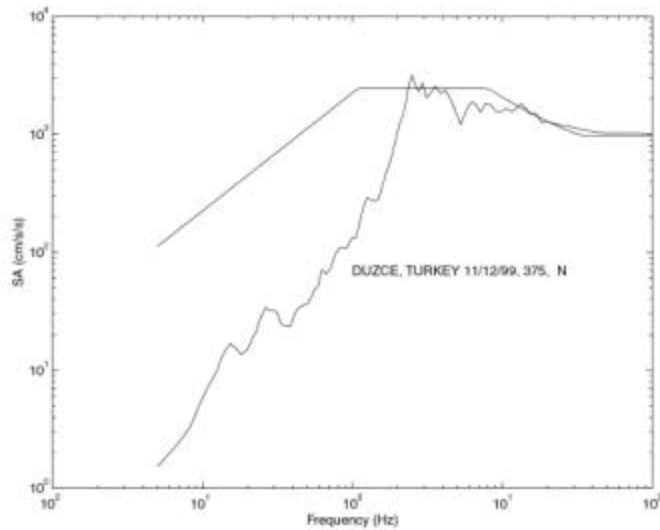


Figure 13d: The acceleration response spectra from recent large earthquakes in Taiwan, Turkey, Japan, and California (see Table 2 for the list of the earthquakes). The figures show only those acceleration response spectra, which have Sa values exceeded the IEEE-693-1997 standard for high seismic performance level.

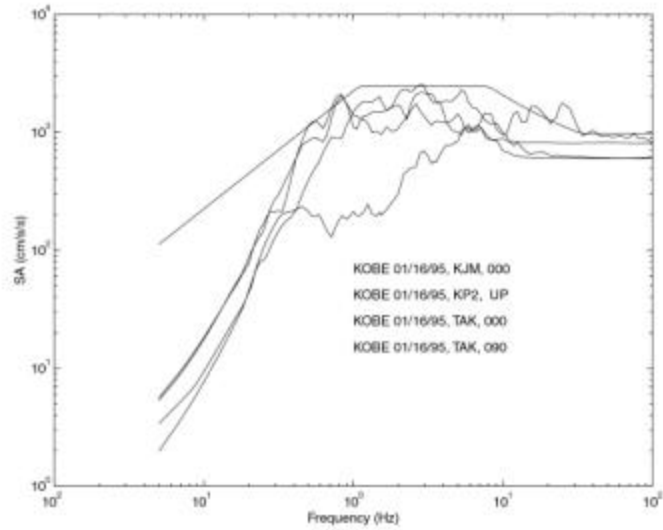


Figure 13e: The acceleration response spectra from recent large earthquakes in Taiwan, Turkey, Japan, and California (see Table 2 for the list of the earthquakes). The figures show only those acceleration response spectra, which have Sa values exceeded the IEEE-693-1997 standard for high seismic performance level.

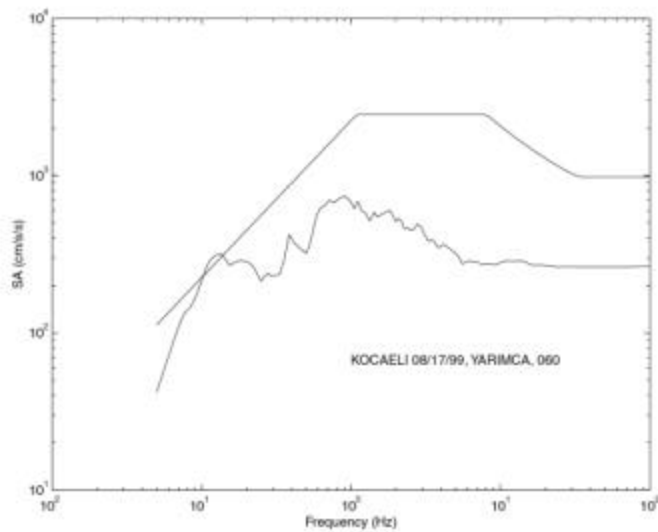


Figure 13f: The acceleration response spectra from recent large earthquakes in Taiwan, Turkey, Japan, and California (see Table 2 for the list of the earthquakes). The figures show only those acceleration response spectra, which have Sa values exceeded the IEEE-693-1997 standard for high seismic performance level.

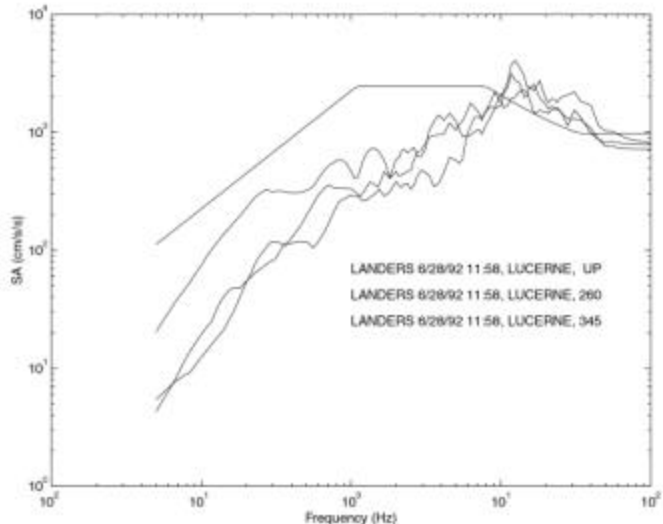


Figure 13g: The acceleration response spectra from recent large earthquakes in Taiwan, Turkey, Japan, and California (see Table 2 for the list of the earthquakes). The figures show only those acceleration response spectra, which have Sa values exceeded the IEEE-693-1997 standard for high seismic performance level.

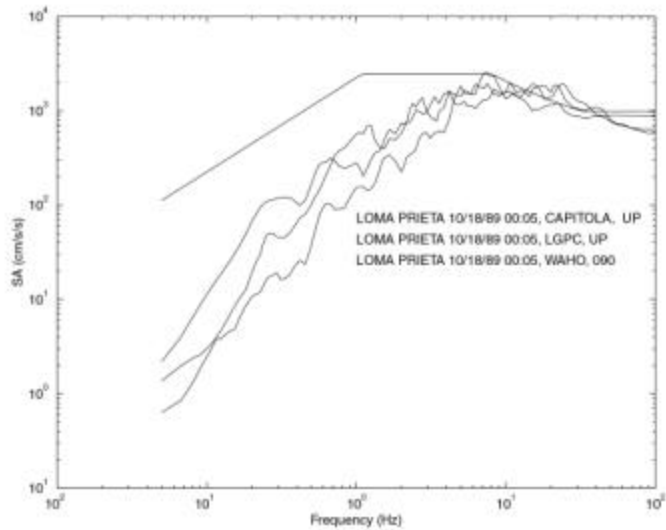


Figure 13h: The acceleration response spectra from recent large earthquakes in Taiwan, Turkey, Japan, and California (see Table 2 for the list of the earthquakes). The figures show only those acceleration response spectra, which have Sa values exceeded the IEEE-693-1997 standard for high seismic performance level.